Journal of Neuroscience Methods

# "Can interhemispheric desynchronization of cerebral blood flow anticipate upcoming vasospasm in aneurysmal subarachnoid haemorrhage patients?"

Michał M. Placek[1,2,*], Peter Smielewski[2], Paweł Wachel[3], Karol P. Budohoski[2], Marek Czosnyka[2], and Magdalena Kasprowicz[1]

1. Department of Biomedical Engineering, Faculty of Fundamental Problems of Technology, Wrocław University of Science and Technology; Wybrzeże S. Wyspiańskiego 27, 50-370 Wrocław, Poland
2. Division of Neurosurgery, Department of Clinical Neurosciences, University of Cambridge; Hills Road, Cambridge CB2 0QQ, United Kingdom
3. Department of Control Systems and Mechatronics, Faculty of Electronics, Wrocław University of Science and Technology; Wybrzeże S. Wyspiańskiego 27, 50-370 Wrocław, Poland

[*]corresponding author: michal.placek@pwr.edu.pl

## Abstract

### Background

Asymmetry of cerebral autoregulation (CA) was demonstrated in patients after aneurysmal subarachnoid haemorrhage (aSAH). A classical method for CA assessment requires simultaneous measurement of both arterial blood pressure (ABP) and cerebral blood flow velocity (CBFV). In this study, we have proposed a cerebral blood flow asymmetry index based only on CBFV and analysed its association with the occurrence of vasospasm after aSAH.

### New method

The phase shifts (PS) between slow oscillations in left and right CBFV (*side-to-side PS*) and between ABP and CBFV (*CBFV–ABP PS*) were estimated using multichannel matching pursuit (MMP) and cross-spectral analysis.

### Results

We retrospectively analysed data collected from 45 aSAH patients (26 with vasospasm). Data were analysed up to 7th day after aSAH unless the vasospasm was detected earlier. A progressive asymmetry, manifested by a gradual increase in *side-to-side PS* on consecutive days after aSAH, was observed in patients who developed vasospasm ($R^2_{\mathrm{adj}} = 0.14$, $p = 0.009$). In these patients, early *side-to-side PS* was more positive than in patients without vasospasm (2.8° ± 5.6° vs –1.7° ± 5.7°, $p = 0.011$). No such a difference was found in *CBFV–*

*ABP PS*. Patients with positive *side-to-side PS* were more likely to develop vasospasm than patients with negative *side-to-side PS* (21/7 vs 5/12, $p = 0.0047$).

### Comparison with existing method

MMP, in contrast to the spectral approach, accounts for non-stationarity of analysed signals. MMP applied to the PS estimation reflects the cerebral blood flow asymmetry in aSAH better than the spectral analysis.

### Conclusions

Changes in *side-to-side PS* might be helpful to identify patients who are at risk of vasospasm.

**Keywords:** transcranial Doppler ultrasonography, multichannel matching pursuit, cerebral vasospasm, interhemispheric asymmetry, cerebral autoregulation, aneurysmal subarachnoid haemorrhage, time-frequency analysis, phase shift

## 1. Introduction

Previous studies showed that after acute brain injury interhemispheric difference in indices describing cerebral blood flow (CBF) are linked to unfavourable outcomes [1–4]. Cerebral autoregulation (CA), which is a closed-loop mechanism of CBF stabilization, was found to be worse on the side of brain lesion and interhemispheric difference in CA was associated with fatal outcome after head injury [1, 2]. Asymmetry of CA was also demonstrated in patients who suffered from aneurysmal subarachnoid haemorrhage (aSAH), and it was found to be related to delayed cerebral ischemia. Interestingly, unfavourable outcome was linked to bilateral dysautoregulation with low asymmetry in this group of patients [3].

A classical method for CA assessment is an analysis of changes in phase shift (PS) calculated between slow waves of arterial blood pressure (ABP) and transcranial Doppler (TCD) cerebral blood flow velocity (CBFV). A cross-spectral analysis [5] is usually used to estimate the PS. A limitation of this spectral method is that it assumes stationarity, whereas CA is recognized to be a non-stationary mechanism [6], and also spontaneous slow waves of ABP and CBFV manifest time-varying behaviour [7]. For these reasons, such an approach may lead to unreliable results.

Furthermore, traditional approach for CA evaluation requires two signals to be simultaneously measured: ABP and CBFV. There are some cases when invasive measurement of ABP is not feasible due to contraindications to arterial cannulation such as: proximal arterial obstruction, coagulopathy, or Reynaud's syndrome. In such cases, a non-invasive measurement of ABP can be considered as a surrogate of direct intra-arterial measurement; however, it is less accurate than the invasive one.

In this study, we have proposed a novel asymmetry index, *side-to-side PS*, that is estimated between slow waves of left and right CBFV and excludes ABP from calculations. In order to account for non-stationarity of analysed signals, a time-frequency method of PS estimation based on the multichannel matching pursuit (MMP) algorithm was applied.

We analysed *side-to-side PS* along with traditional *CBFV–ABP PS* (estimated using both cross-spectral analysis and MMP-based method) in patients after an aSAH. We focused on temporal changes of PSs in respect to occurrence of cerebral vasospasm. Results obtained using cross-spectral analysis and MMP-based method were compared.

## 2. Material and methods

### 2.1. Patients and management

In the study, we retrospectively analysed data collected from patients after an aSAH hospitalized at the Division of Neurosurgery in Addenbrooke's Hospital (Cambridge, UK) between 2010 and 2012. The following inclusion criteria applied: age ≥ 18 years, aSAH confirmed with either computed tomography angiography or digital subtraction angiography, time elapsed from ictus less than 5 days. Written informed consent signed by a patient or their next of kin was collected. The patients were treated according to current guidelines [8-10]. Initial treatment included cardiopulmonary support (if required), avoiding hypovolemia, oral nimodipine 60 mg every four hours, and external ventricular drainage to cure acute hydrocephalus (if indicated). Treatment of the culprit aneurysm was with surgical clipping or endovascular embolization. TCD monitoring was performed every few days by a single clinician (K.P.B.) to screen for cerebral vasospasm [8]. The TCD criterion for vasospasm was mean CBFV in the middle cerebral artery > 120 cm/s with a concomitant Lindegaard ratio (the quotient of CBFV in the middle cerebral artery and the extracranial internal carotid artery) > 3 [11]. The prospective study was approved by the local Research Ethics Committee. For current retrospective analysis formal consent was not required. Previously, the clinical material was used to analyse CA in aSAH and the results can be found in [3, 12, 13].

From original database containing 98 aSAH patients, we considered those who had sufficiently long (at least 15 minutes) simultaneous, bilateral TCD monitoring of the middle cerebral arteries. For the purpose of the analysis, the ipsilateral side was deemed the side of vasospasm if vasospasm was present. In patients without vasospasm or with bilateral vasospasm, the ipsilateral side was the side of the culprit aneurysm. Due to this definition, patients with midline aneurysms (the anterior communicating artery and the basilar artery) followed by bilateral or no vasospasm were excluded from the analysis as determination of the ipsilateral side was not possible. In total, 45 patients (35 females and 10 males, age range: 33–81, mean age: 57) were selected to this study, among whom 26 patients developed vasospasm.

If available, ABP was measured invasively from the radial artery by a pressure monitoring device (Baxter Healthcare, Deerfield, IL, USA). Otherwise, it was monitored noninvasively

using a finger plethysmograph (Finapres® 2300, Englewood, CO, USA) with the hand kept steady at heart level. Bilateral CBFV in the middle cerebral arteries was measured via the temporal window at a depth of 45–60 mm using a TCD kit (Doppler-Box™, DWL Compumedics®, Singen, Germany) with an aid of a head positioning device (Lam Rack, DWL Compumedics®). Data were recorded at a sampling frequency of 200 Hz using ICM+® software (Cambridge Enterprise Ltd, Cambridge, UK).

### 2.2. Data pre-processing

Before down-sampling, ABP and CBFV were smoothed using Nadaraya–Watson non-parametric kernel regression estimate [14, 15] in order to filter out higher frequencies [16]. Gaussian kernel was chosen with the smoothing parameter *h* adjusted to removing heart beat and respiration waves, while preserving low frequencies (slow waves) where cerebral autoregulation is active [17]. Smoothed data were then down-sampled with the frequency of 2 Hz.

Decimated time series were divided into 5-minutes long frames with 50% overlap. In each frame, signals were individually detrended by removing the regression line [18]. Next, for consecutive frames, the values of PS were estimated between each pair of signals, i.e. $CBFV_{ipsi}$–ABP, $CBFV_{cont}$–ABP, and $CBFV_{cont}$–$CBFV_{ipsi}$, giving *ipsilateral PS*, *contralateral PS*, and *side-to-side PS*, respectively. Finally, representative PSs for entire recording were calculated as average PSs over all frames.

Data were processed using custom written scripts in MATLAB® (MathWorks®, Natick, MA, USA). These scripts can be found in Appendix A available in the online version of this article.

### 2.3. Estimating phase shift using matching pursuit

The matching pursuit (MP) algorithm with time-frequency dictionaries was introduced by Mallat & Zhang [19]. It enables explaining the content of the analysed signal in the form of the sum of the time functions (called atoms) that are chosen iteratively from a so-called dictionary to adaptively fit to the local signal structures. Gabor functions (sines modulated in amplitude with Gaussian envelopes) are usually used as atoms.

In technical terms, MP decomposes a signal into a linear combination of waveforms belonging to a redundant set of atoms, called the dictionary *D*. The original signal is considered as the 0-th order residuum. The decomposition is performed iteratively. In each iteration, MP selects from *D* the atom that best matches the current residuum, i.e. the atom that maximizes the modulus of the dot product of this atom and the residuum. Since all atoms in *D* have a unit $L^2$ norm, the selected atom is subtracted from the *n*-th order residuum after adjusting its amplitude, which is the value of the dot product. This subtraction yields the $(n + 1)$-th order residuum. The procedure, which is shown in Fig. 1, is repeated on the residua until a stopping criterion is met. A dictionary used in MP typically consists of time-frequency Gabor atoms because they provide optimal joint time-frequency localization [20]. Gabor

atoms are functions of time, $g_\gamma$, parametrized by $\gamma = (\tau, \omega, \sigma)$, where $\tau$, $\omega$, and $\sigma$ denote translation, modulation, and dilation, respectively:

$$g_\gamma(t) = K(\gamma) \exp\left(-\pi\left(\frac{t-\tau}{\sigma}\right)^2 + j\omega t\right), \tag{1}$$

where $K(\gamma)$ is such that $\|g_\gamma\| = 1$, $j$ stands for imaginary unit, and $\|\cdot\|$ denotes $L^2$ norm.

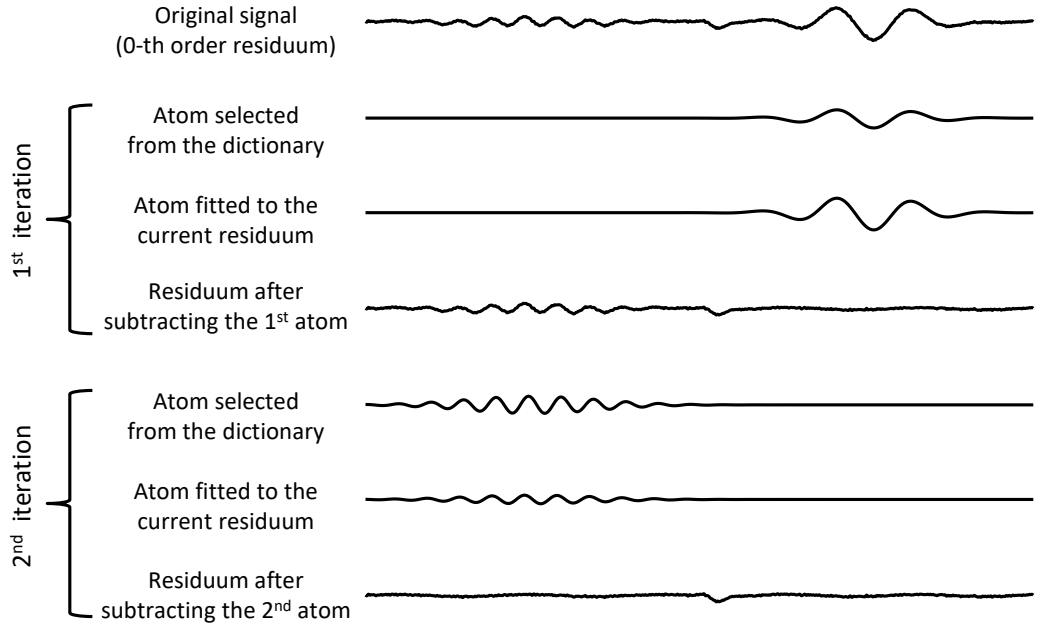


**Fig. 1** The matching pursuit decomposition of an illustrative signal. Two iterations of the algorithm are shown.

The main goal of the multichannel matching pursuit (MMP) is to decompose a multichannel signal using the same set of atoms. There are several ways to extend MP to a multichannel case [21, 22]. In the paper, we consider a variant which seeks the time-frequency atoms that must have the same $\gamma$ but can have different amplitudes and phases across channels. The criterion for selecting the atom which best matches the residuum of the multichannel signal was defined as the maximal sum of squared moduli of dot products of the residuum in each channel and the atom [21, 23, 24]. Denoting the decomposed *m*-channel signal as $\boldsymbol{f} = (f_1(t), f_2(t), \ldots, f_m(t))$, the *n*-th order residuum as $R^n\boldsymbol{f}$, the atom fitted in the *n*-th iteration as $g_{\gamma_n}$, and the dot product by $\langle\cdot,\cdot\rangle$, the procedure is defined in the following way:

$$\begin{cases} R^0\boldsymbol{f} = \boldsymbol{f} \\ g_{\gamma_n} = \arg\max_{g_\gamma \in D} \sum_{i=1}^{m} \left|\langle R^n f_i, g_\gamma\rangle\right|^2. \\ R^{n+1}\boldsymbol{f} = R^n\boldsymbol{f} - \langle R^n\boldsymbol{f}, g_{\gamma_n}\rangle g_{\gamma_n} \end{cases} \tag{2}$$

The MP decomposition can be performed in real [21, 22] or complex domain [24, 25]. Since the complex-domain approach operates on analytic signals, real-valued sequences need to be converted by the Hilbert transform. The advantage of the complex-domain approach is

that both amplitude and phase of the fitted Gabor atom are contained in its complex weight [24], whereas in the real-domain approach, only amplitude is contained in the weight of the real-valued atom function but its phase must be found in an additional step [22]. Since in our work estimation of PS is crucial, we employed the complex-domain approach.

To estimate PSs between a given pair of signals (i.e. $CBFV_{ipsi}$–ABP, $CBFV_{cont}$–ABP, or $CBFV_{cont}$–$CBFV_{ipsi}$), a two-channel matching pursuit decomposition was applied[1] (hence $m = 2$). Before the decomposition, each of the two channels was normalised so as to have a unit $L^2$ norm. This was done to prevent a situation where the channel with the higher norm has greater influence on selecting the atoms of the decomposition.

Local PSs, $\varphi_n$, between the two channels can be retrieved from the complex weights $w_{n,1} = \langle R^n f_1, g_{\gamma_n} \rangle$ and $w_{n,2} = \langle R^n f_2, g_{\gamma_n} \rangle$ of the atom fitted in the *n*-th iteration:

$$\varphi_n = \arg\left(\frac{w_{n,1}}{w_{n,2}}\right) = \arg\left(\frac{\langle R^n f_1, g_{\gamma_n} \rangle}{\langle R^n f_2, g_{\gamma_n} \rangle}\right), \tag{3}$$

where $\arg(\cdot)$ stands for the argument of the complex number, bounded to the interval $(-\pi, \pi]$. The sign of PS was assumed in accordance with the convention that PS between CBFV and ABP is positive when CBFV leads ABP in phase [26]. In turn, *side-to-side PS* was assumed positive when $CBFV_{cont}$ leads $CBFV_{ipsi}$. Fig. 2 visualizes the PS calculation process according to Eq. (3).

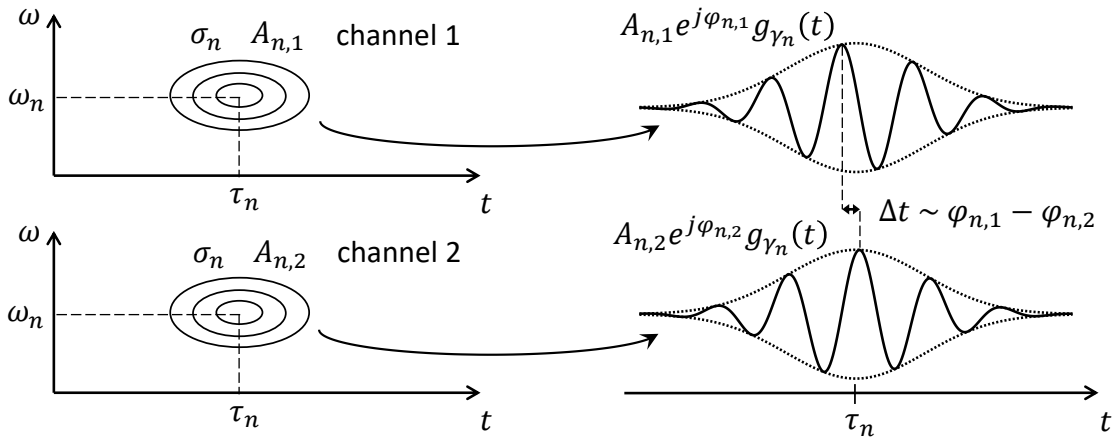


**Fig. 2** Local phase shift can be calculated for a common atom fitted by multichannel matching pursuit to the signals of the two channels. Oscillatory features in the two measured signals are associated with a Gabor atom (sinusoid modulated in amplitude with Gaussian envelope). Only the amplitude, $A_{n,i}$, and phase, $\varphi_{n,i}$, of the fitted atom can differ across the two channels, $i = 1, 2$. Since the atom selected in a given iteration has the same translation, $\tau_n$, modulation, $\omega_n$, and dilation, $\sigma_n$, these oscillatory time courses are coherent, and therefore phase shift between them can be estimated. Due to the properties of complex numbers, this phase shift can be derived from Eq. (3).

[1] It is also feasible to perform a three-channel matching pursuit with bilateral CBFV and ABP decomposed all together; however, it is beyond the scope of this paper.

In the current application, the dictionary $D$ consisted of Gabor atoms such that $\omega/(2\pi) < 0.1$ Hz and $\sigma > 15$ seconds in order to avoid the influence of faster oscillations and potential short-lasting changes which are unlikely to bear useful physiological information related to the mechanisms responsible for adjustment of CBF. Moreover, a lower number of atoms in the dictionary implies faster computations. Parameters $\gamma$ of the atoms included in the dictionary $D$ were chosen from oversampled dyadic sequences [19], taking into account abovementioned restrictions.

Local PSs corresponding to consecutive atoms were then averaged to obtain the resulting value of MMP-derived phase shift ($PS_{MMP}$) between the two signals of the two channels:

$$\varphi = \frac{1}{N}\sum_{n=1}^{N} \varphi_n. \quad (4)$$

The number of iterations of the MMP decomposition was limited to $N = 20$.

## 2.4. Spectral phase shift

The spectral phase shift ($PS_{sp}$) was also calculated between $CBFV_{ipsi}$ and ABP, $CBFV_{cont}$ and ABP, as well as $CBFV_{cont}$ and $CBFV_{ipsi}$. Like in the MMP approach, each monitoring session was first divided into 5-minutes long 50% overlapped data frames.

For each data frame, $PS_{sp}$, along with magnitude-squared coherence, was estimated using the Welch's overlapped averaged periodogram method [27] with five 100-seconds long Hanning-windowed data segments. Obtained cross- and auto-spectra were additionally smoothed by convolving them with the window (¼, ½, ¼) prior to calculating coherence and phase spectrum, as recommended in [5]. The threshold for significant magnitude-squared coherence was established at the level of 0.39 on the basis of Monte Carlo simulations [5]. The resulting value of $PS_{sp}$ was estimated as a mean phase over those frequencies below 0.1 Hz for which coherence was above the threshold [28]. If coherence was persistently low across all the considered frequency band for a given data frame, $PS_{sp}$ was not evaluated. Finally, the average representative $PS_{sp}$ for the entire recording was calculated.

## 2.5. Statistical analysis

### 2.5.1. Analysis of differences in phase indices and other haemodynamic parameters

Patients were dichotomized in respect to occurrence of vasospasm. Data were analysed up to 7th day after aSAH [29] in both groups of patients with and without vasospasm, unless the vasospasm was detected earlier, in which case data recorded during the vasospasm were excluded from the analysis. The values of the parameters corresponding to repeated recordings were averaged so as to obtain one representative value per patient. In the group of patients with vasospasm, we also calculated mean values of the considered parameters for the period of vessel narrowing (during vasospasm). The parameters were normally distributed based on the Kolmogorov–Smirnov test at a significance level of 0.05. Subsequently, parametric tests were chosen. The *t*-test for independent samples was used to compare mean values of the parameters between different groups of patients, i.e. those who developed

vasospasm vs those who did not. Paired *t*-test was employed to compare the parameters obtained from patients who developed vasospasm at baseline vs during vessels narrowing as well as on ipsilateral vs contralateral side. Finally, one-sample *t*-test was used to check whether *side-to-side PS*s were significantly different than zero.

#### 2.5.2. Analysis of temporal changes in phase indices using mixed-effects model

Association between PSs and time in the first seven days after aSAH was assessed using linear mixed-effects models [30]. The models were fitted independently for data coming from patients who later developed vasospasm (only data before vasospasm occurred were analysed) and those who did not. Day number after aSAH was treated as a fixed-effects term, whereas patient's ordinal number as a random-effects term. Varying intercept with fixed slope, instead of varying slope, was selected for the random-effect, since some patients had low number of recording sessions in considered days after aSAH. Furthermore, the fixed slope model is sufficient when the main goal of fitting is to investigate general trend of PSs changes in time.

From fitted models, we obtained adjusted $R^2$ ($R^2_{\text{adj}}$) and *p*-value. $R^2_{\text{adj}}$ is a proportion of variability in the response explained by the fitted model adjusted for the number of fixed-effects coefficients. Namely, $R^2_{\text{adj}} = 1 - \frac{SSE}{SST} \cdot \frac{n-1}{n-k}$, where *SSE* is the sum of squared conditional residuals, *SST* is the sum of squared deviations of the observed response values from their mean, *n* is the total number of observations, and *k* is the number of fixed-effects coefficients. The significance (*p*-value) of association between given PS index and time was obtained by the *F*-test with the null hypothesis assuming that the coefficient representing fixed-effects term is zero.

#### 2.5.3. Association between *side-to-side PS* and occurrence of vasospasm

To check whether *side-to-side PS* has a potential to dichotomize patients in respect to occurrence of vasospasm, we averaged *side-to-side PS* calculated in initial days after aSAH for each patient. Then, a receiver operating characteristic curve was used to find the optimal value of threshold for *side-to-side PS*. The relationship between the binary (thresholded) parameter and the presence or absence of vasospasm were compared using the Fisher's exact test.

Statistical analysis was performed using Statistics and Machine Learning Toolbox in MATLAB® R2017a.

## 3. Results

### 3.1. Differences between mean values of parameters

Table 1 shows values of physiological parameters in early days after aSAH in the two groups of patients.

**Table 1** Physiological parameters dichotomized by occurrence of cerebral vasospasm

| Parameter | Non-spasm ($n$ = 19) | Pre-spasm ($n$ = 26) | $p$-value |
|---|---|---|---|
| Ipsilateral CBFV (cm/s) | 59.5 ± 22.1 | 81.4 ± 26.2 | **0.005** |
| Contralateral CBFV (cm/s) | 60.7 ± 20.1 | 70.8 ± 30.1 | 0.21 |
| Ipsilateral $PS_{MMP}$ (deg) | 13.0 ± 10.2 | 13.2 ± 9.5 | 0.96 |
| Contralateral $PS_{MMP}$ (deg) | 12.8 ± 13.1 | 13.5 ± 13.9 | 0.85 |
| Side-to-side $PS_{MMP}$ (deg) | –1.7 ± 5.7 | 2.8 ± 5.6 | **0.011** |
| Ipsilateral $PS_{sp}$ (deg) | 32.8 ± 21.6 | 27.5 ± 17.4 | 0.37 |
| Contralateral $PS_{sp}$ (deg) | 34.6 ± 21.1 | 29.1 ± 18.3 | 0.36 |
| Side-to-side $PS_{sp}$ (deg) | –3.2 ± 14.1 | 2.2 ± 16.2 | 0.25 |

Results are: mean ± standard deviation. $p$-values were calculated using $t$-test for independent samples (non-spasm vs pre-spasm). Statistically significant $p$-values are given in bold. Subscripts $_{MMP}$ and $_{sp}$ refer to the method used to estimate phase shift (PS): multichannel matching pursuit or spectral analysis, respectively. Patients were dichotomized by the occurrence of cerebral vasospasm. The term 'pre-spasm' refers to data collected up to 7th day after aSAH in patients who later developed vasospasm, excluding cases when vasospasm had already occurred.

A comparison between the values of physiological parameters at baseline (before vasospasm was detected) vs during vasospasm is presented in Table 2. The total number of compared patients was $n$ = 21 because five patients were excluded from the analysis due to lack of sufficiently long, bilateral CBFV recording during vasospasm. We also tested whether parameters on the ipsilateral side were different than those on the contralateral side and whether *side-to-side PS* was significantly different than zero. At baseline, there were no differences between the ipsilateral and the contralateral PSs. Only during vasospasm did ipsilateral PSs become significantly lower than contralateral PSs. Nevertheless, *side-to-side* $PS_{MMP}$ was already significantly different than zero at baseline. Such an observation was not found in patients who did not develop vasospasm ($p$ = 0.22).

**Table 2** Physiological parameters before vs during vasospasm (21 patients)

| Parameter | Pre-spasm | During spasm | *p*-value |
|---|---|---|---|
| Ipsilateral CBFV (cm/s) | 77.6 ± 27.1 | 161.0 ± 42.9 | **$< 10^{-7}$** |
| Contralaeral CBFV (cm/s) | 69.0 ± 32.3 | 88.9 ± 31.4 | **0.002** |
| Ipsi- vs contralaeral CBFV (*p*-value) | **0.027** | **$< 10^{-6}$** | |
| Ipsilateral $PS_{MMP}$ (deg) | 14.2 ± 9.3 | 6.8 ± 7.9 | **0.009** |
| Contralateral $PS_{MMP}$ (deg) | 15.5 ± 13.2 | 12.2 ± 9.2 | 0.26 |
| Ipsi- vs contralateral $PS_{MMP}$ (*p*-value) | 0.52 | **0.028** | |
| Side-to-side $PS_{MMP}$ (deg) | 3.5 ± 5.6 | 8.0 ± 5.4 | **0.032** |
| Side-to-side $PS_{MMP}$ vs zero (*p*-value) | **0.0095** | **$< 10^{-4}$** | |
| Ipsilateral $PS_{sp}$ (deg) | 28.4 ± 19.1 | 13.3 ± 15.0 | **0.008** |
| Contralateral $PS_{sp}$ (deg) | 31.1 ± 18.7 | 25.7 ± 19.1 | 0.21 |
| Ipsi- vs contraletral $PS_{sp}$ (*p*-value) | 0.46 | **0.012** | |
| Side-to-side $PS_{sp}$ (deg) | 2.2 ± 15.5 | 17.9 ± 21.2 | **0.007** |
| Side-to-side $PS_{sp}$ vs zero (*p*-value) | 0.53 | **0.001** | |

Results are: mean ± standard deviation. *p*-values were calculated using either *t*-test for dependent samples (pre-spasm vs during spasm and ipsilateral vs contralateral) or one-sample *t*-test (whether side-to-side phase shift is different than zero). Statistically significant *p*-values are given in bold. Subscripts $_{MMP}$ and $_{sp}$ refer to the method used to estimate phase shift (PS): multichannel matching pursuit or spectral analysis, respectively. The term 'pre-spasm' refers to data collected up to 7th day after aSAH in patients who later developed vasospasm, excluding cases when vasospasm had already occurred.

### 3.2. Association between phase-indices and days after aSAH

In the group of patients who developed vasospasm, *side-to-side* $PS_{MMP}$ and *contralateral* $PS_{MMP}$ exhibited significant association with time expressed in days after aSAH ($R^2_{adj} = 0.14$, $p = 0.009$ and $R^2_{adj} = 0.19$, $p = 0.002$, respectively). No relationship was found between *ipsilateral* $PS_{MMP}$ and time after aSAH. On the other hand, in the group of patients without vasospasm no significant association between $PS_{MMP}$ in respect to time was observed (Fig. 3). No relationships between $PS_{sp}$ (*ipsilateral*, *contralateral*, and *side-to-side*) and time after aSAH were found in either of patient groups.

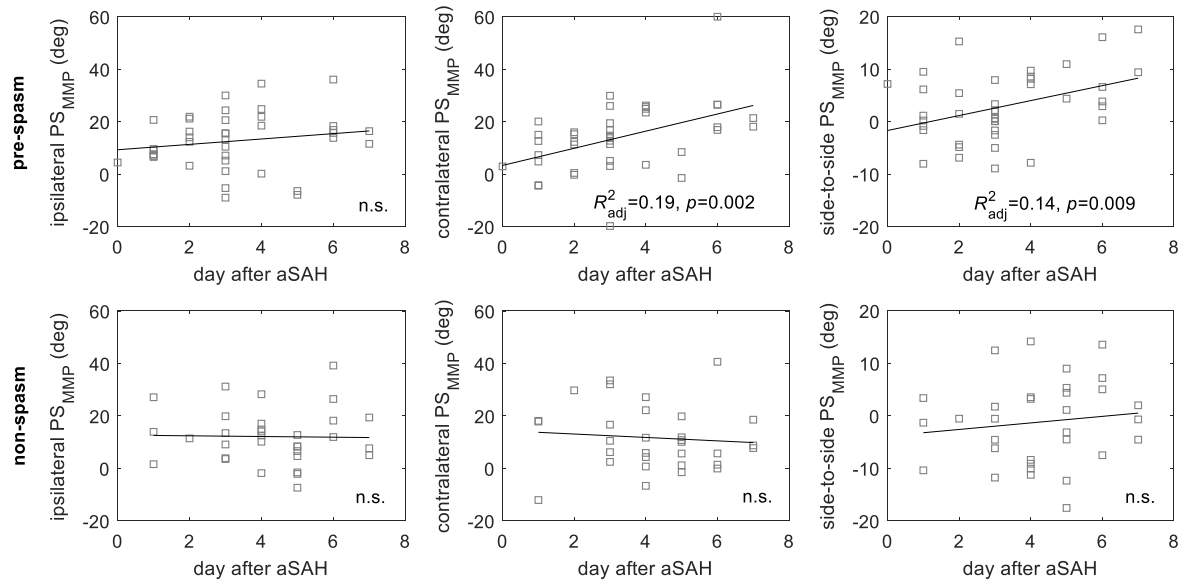


**Fig. 3** Upper row contains time profiles of phases shifts (ipsilateral, contralateral, and side-to-side) obtained in the group of patients who later developed vasospasm. Data recorded when vasospasm had already been detected in a given patient were not considered. Lower row shows temporal fluctuations of phases shifts obtained in the group of patients who did not developed vasospasm. Each point corresponds to a single recording session.

### 3.3. Relationship between early asymmetry and the presence of vasospasm

A receiver operating characteristic analysis showed that *side-to-side* $PS_{MMP}$ had a potential to predict vasospasm (area under the curve: 0.72). The optimal value of threshold was 0° with sensitivity and specificity of 0.81 and 0.63, respectively. The Fisher's exact test confirmed statistical significance of the relationship between thresholded *side-to-side* $PS_{MMP}$ and the presence or absence of vasospasm ($p$ = 0.0047; Fig. 4).

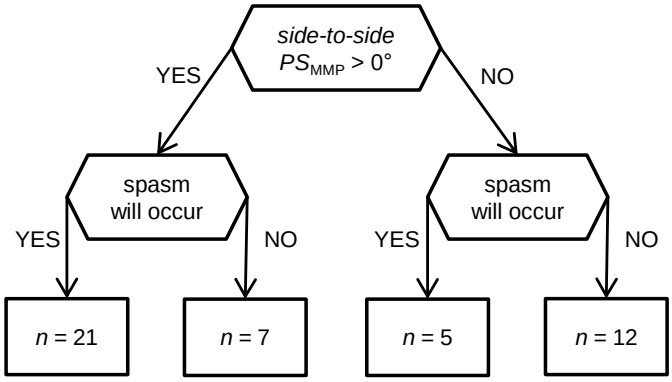


**Fig. 4** Diagram illustrating the relationships between early asymmetry and the occurrence of vasospasm. The number *n* of patients falling in each category is given.

## 4. Discussion

### 4.1. Interpretation of the results

In this study, a novel TCD-based parameter named *side-to-side PS* was applied to investigate the temporal changes in asymmetry of CBF in aSAH patients. A progressive desynchronization — manifested by a gradual increase in the *side-to-side* $PS_{MMP}$ in

subsequent days after aSAH — was found in patients who later developed vasospasm. Such a correlation was not found in patients who did not demonstrate vessel narrowing in the following days after ictus.

When patients with and without vasospasm were compared in early days after aSAH, higher (more positive) *side-to-side* $PS_{MMP}$ was found in those patients who later demonstrated vessel narrowing. This positive value of *side-to-side PS* means that slow oscillations of $CBFV_{ipsi}$ are delayed in respect to $CBFV_{cont}$. This may suggest that CA on the ipsilateral side is worse than on the contralateral side in early days after aSAH. However, no significant differences between *ipsilateral PS* and *contralateral PS* were found at baseline. On the other hand, *side-to-side* $PS_{MMP}$ was significantly different from zero before vasospasm occurred, suggesting that early asymmetry is present before vessel narrowing. Furthermore, patients who had positive *side-to-side* $PS_{MMP}$ presented vasospasm more often than patients with negative *side-to-side* $PS_{MMP}$ or no asymmetry (based on the Fisher's exact test). These observations resulted from the MMP analysis.

Along with *side-to-side PS*, temporal changes in CA indices were analysed. There was no relationship between time after aSAH and *ipsilateral PS* estimated using either MMP or spectral method. There was, however, a gradual increase in *contralateral* $PS_{MMP}$ vs initial days after bleeding. The fact that *contralateral* $PS_{MMP}$ significantly positively correlated with time is difficult to interpret. It may suggest gradual recovery of CA in early days after aSAH. However, not observing similar pattern in the group of patients who did not develop vasospasm seems to contradict this hypothesis. Another explanation might be that the sample size analysed in our study was relatively small and therefore the correlation found between *contralateral* $PS_{MMP}$ and time after aSAH might be a specious result. The *ipsilateral PS*s (both MMP and spectral) significantly decreased during vasospasm, suggesting disturbed CA, as expected [31].

To investigate relationships between considered indices and occurrence of vasospasm, we used relatively simple tools, like linear mixed-effects models. In terms of alternative approaches, machine learning models could be used to find additional predictive features [32]. More complex machine learning models, however, require larger study sample and might not be straightforward in interpretation.

## 4.2. Methodological considerations

Methods which account for non-stationarity appear to be more adequate to study CBFV–ABP relationship. Models based on autoregressive moving-average [33-35] and recursive least squares adaptive filter [36, 37] offered better time resolution and more in-depth insight into the dynamic nature of CA during changes in $CO_2$ concentration. Employing time-frequency analysis allowed to reduce dispersion of CBFV–ABP phase estimates and avoid data rejection in case low spectral coherence was encountered [7].

In this study, applying MMP allowed identifying asymmetry of CBF in patients who later developed vasospasm. Such an asymmetry was not found when the spectral method was used.

This might be related to the fact that MMP led to lower dispersion of *side-to-side PS* estimates than the spectral method. It means that inter-subject variability of *side-to-side* $PS_{MMP}$ was lower and hence its ability to differentiate between patients with and without spasm was higher.

*Side-to-side PS* defined as a PS between CBFV oscillations shows asymmetry but it is not clear how it relates to CA. Before vasospasm occurred, *side-to-side PS* was mildly positive and there was no difference between *ipsilateral* and *contralateral PS*. During vasospasm, *side-to-side PS* increased and the difference between *ipsilateral* and *contralateral PS* became significant. This suggests that even though *side-to-side PS* is calculated independently of ABP, it may reflect asymmetry of CA. However, *side-to-side PS* might be calculated from a frequency band (or time-frequency regions for MMP) different than one for either *contralateral PS* or *ipsilateral PS* (see Fig. 5). This is related to the methodological restriction of considering PS in frequencies where coherence exceeds the threshold (or in coherent time-frequency MMP atoms).

Another possible way to characterize asymmetry is to consider the difference between *contralateral* and *ipsilateral PS*. This definition, however, does not eliminate ABP from calculations. Furthermore, subtracted *contralateral* and *ipsilateral PS*s might be calculated from different frequency bands (see Fig. 5). This may lead to unreliable estimates of asymmetry because it has been shown that CA is the frequency-dependent mechanism and *consequently CBFV–ABP PS* decreases, on average, with the frequency [38, 39].

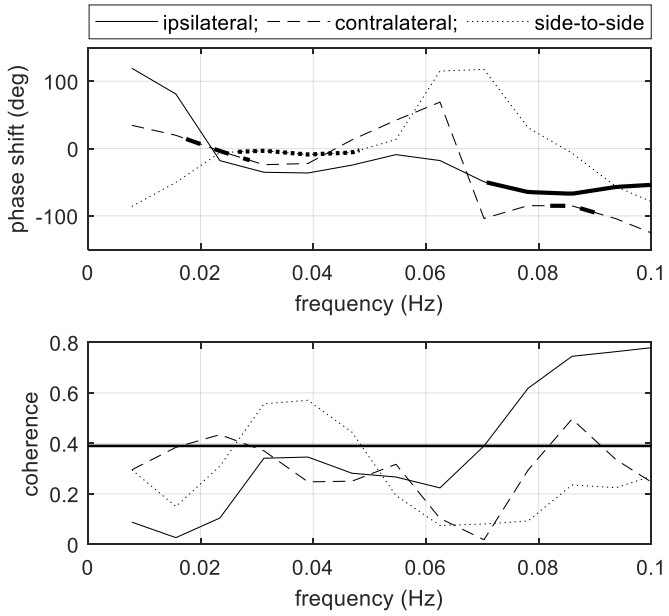


**Fig. 5** Phase and coherence spectra obtained from cross-spectral analysis for an illustrative data frame. Thickened parts of phase spectra relate to frequencies where the corresponding coherence was above the 0.39 threshold. Due to the methodological restriction, only those parts of phase spectra are taken to estimate the resulting value of phase shift. Consequently, ipsilateral, contralateral, and side-to-side phase shifts might be calculated from different frequency bands, depending on the corresponding coherence spectra.

Since we wanted to investigate whether the asymmetry of cerebral blood flow in early days after aSAH is associated with the occurrence of vasospasm, we decided to focus on first seven days after aSAH unless the vasospasm was detected earlier, in which case data recorded during the vasospasm were excluded from the analysis. In the considered study sample, the majority of patients with vasospasm experienced it within first 7 days after aSAH. For that reason, there were too few data points corresponding to days later than the 7th day after aSAH to perform reliable statistical analyses involving this group of patients.

In order to ensure validity of phase estimation, many methods which produce PS also use auxiliary measure like coherence, e.g. spectral coherence [5], time-frequency coherence [7], or wavelet coherence [40]. The MMP method presented in this work does not directly use coherence to control validity of estimated PS between two signals. Ideally, the process of decomposition should select atoms which are coherent across both channels. A high number of iterations, however, increases the risk that selected atoms might be 'overfitted.' Particularly, it can happen that some atom was selected because its dot product was high only for one channel, while the dot product for the other channel was close to zero. In that case, PS defined by Eq. (3) is not reliable due to singularity. This is similar to estimating PS by the cross-spectral analysis when coherence between two signals is close to zero [41]. The MMP is a greedy algorithm [19, 20]. In each iteration, it selects from the dictionary the atom that best matches the current residuum of the signal according to Eq. (2). This strategy, in general, yields a reasonable decomposition but not optimal, in particular, in the mean-squared sense [42].

Another problem related to a high number of iterations is that it increases time cost of MMP. One the other hand, if the number of selected atoms is small, the resultant PS is estimated from a small part of the time-frequency plane and hence may not be representative. For this reason, the number of fitted atoms in MMP has a substantial influence on the resulting value of PS. Taking into account the abovementioned pros and cons, the number of atoms was experimentally fixed to $N = 20$, which corresponded to explaining, on average, about 96% of energy in single 5-minutes long frame of analysed signals by fitted atoms.

One must remember that data pre-processing may influence the final value of phase estimates. This is particularly important in the context of greediness of the MMP algorithm. In the presented method, smoothing strength was adjusted to removing heart beat and respiration waves, while preserving slow waves. Additionally, atoms in the MMP dictionary as well as the spectral analysis were limited up to 0.1 Hz. Smoothed data were down-sampled with the frequency of 2 Hz. Since we focused on analysing fluctuations up to 0.1 Hz, the sampling frequency of 2 Hz gives a sufficient safety margin. It also reduces execution time of the MMP algorithm to acceptable level. Since analysed recording varied in duration, they were divided into 5-minutes long frames and processed individually. This approach allowed, among others, using exactly the same dictionary in the MMP algorithm for all data frames. In consequence, it was reasonable to set the fixed number of MMP iterations for all of analysed recordings. Detrending, i.e. removal of linear trend in each 5-minutes long data frame, was performed for

two reasons. Firstly, the DC component and potential linear trend do not bear physiologically relevant information. Secondly, the presence of linear trend may impede the MMP decomposition, as Gabor atoms in the dictionary are free from linear trend.

### 4.3. Limitations

In our data cohort, the arterial partial pressure of carbon dioxide ($PaCO_2$) was not measured, although no significant changes in $PaCO_2$ were performed during data recording. It has been shown, however, that a multivariate approach to describe changes in CBFV that includes not only ABP but also $CO_2$ concentration (or its end-tidal value) is more accurate than the univariate model [17, 43, 44]. Further study using the MMP method is needed to determine the effect of $PaCO_2$ changes on the CBF asymmetry assessment by *side-to-side PS*.

We excluded from our analysis patients who did not exhibit substantial interhemispheric differences, i.e. those who had midline aneurysm followed by bilateral or no vasospasm. Moreover, to select the ipsilateral side for each patient, we used information about the side of vasospasm if it occurred. Even though we focused on data recorded before a vasospasm was diagnosed, using information about the side of vasospasm may impede clinical implementation of *side-to-side PS*.

## 5. Conclusions

In this study, we have proposed a novel asymmetry index, *side-to-side PS*, that is estimated between slow waves of left and right CBFV and excludes ABP from calculations. The presented method allowed to observe gradually increasing asymmetry of CBF in subsequent days after aSAH in patients who later developed vasospasm and that they had higher *side-to-side* $PS_{MMP}$ than those who did not demonstrate vessel narrowing. The study shows that early changes in *side-to-side* $PS_{MMP}$ might be helpful to identify those patients who are at risk of vasospasm. MMP applied to the PS estimation reflects the asymmetry of CBF better than the conventional spectral analysis.

## Acknowledgments

The authors would like to thank Dr Artur Matysiak for sharing MATLAB functions for the multichannel matching pursuit and Dr Cezary Sielużycki for discussions on applications of the matching pursuit algorithm. M. M. Placek was a recipient of the ETIUDA scholarship from the National Science Centre, Poland (grant no 2017/24/T/ST7/00233).

## Conflict of interest

ICM+® software is licensed by Cambridge Enterprise Ltd, Cambridge, UK (https://icmplus.neurosurg.cam.ac.uk). P. Smielewski and M. Czosnyka have a financial interest in a fraction of the licensing fee.

## Appendix A. Supplementary data

Supplementary material related to this article can be found, in the online version, at doi: https://doi.org/10.1016/j.jneumeth.2019.108358. It contains MATLAB scripts with sample data used in this study.

## References

[1] Schmidt EA, Czosnyka M, Smielewski P, Piechnik S, Pickard J. Asymmetry of cerebral autoregulation following head injury. Intracranial Pressure and Brain Biochemical Monitoring: Springer; 2002. p. 133–4.

[2] Schmidt EA, Czosnyka M, Steiner LA, Balestreri M, Smielewski P, Piechnik SK, et al. Asymmetry of pressure autoregulation after traumatic brain injury. Journal of neurosurgery. 2003;99:991–8.

[3] Budohoski KP, Czosnyka M, Kirkpatrick PJ, Reinhard M, Varsos GV, Kasprowicz M, et al. Bilateral failure of cerebral autoregulation is related to unfavorable outcome after subarachnoid hemorrhage. Neurocritical care. 2015;22:65–73.

[4] Kumar A, Schmidt E, Hiler M, Smielewski P, Pickard J, Czosnyka M. Asymmetry of critical closing pressure following head injury. Journal of Neurology, Neurosurgery & Psychiatry. 2005;76:1570–3.

[5] Claassen JA, Meel-van den Abeelen AS, Simpson DM, Panerai RB. Transfer function analysis of dynamic cerebral autoregulation: A white paper from the International Cerebral Autoregulation Research Network. Journal of Cerebral Blood Flow & Metabolism. 2016;36:665–80.

[6] Panerai RB. Nonstationarity of dynamic cerebral autoregulation. Medical Engineering & Physics. 2014;36:576–84.

[7] Placek MM, Wachel P, Iskander DR, Smielewski P, Uryga A, Mielczarek A, et al. Applying time-frequency analysis to assess cerebral autoregulation during hypercapnia. PLOS ONE. 2017;12:e0181851.

[8] Connolly Jr ES, Rabinstein AA, Carhuapoma JR, Derdeyn CP, Dion J, Higashida RT, et al. Guidelines for the management of aneurysmal subarachnoid hemorrhage: a guideline for healthcare professionals from the American Heart Association/American Stroke Association. Stroke. 2012;43:1711–37.

[9] Komotar RJ, Schmidt JM, Starke RM, Claassen J, Wartenberg KE, Lee K, et al. Resuscitation and critical care of poor-grade subarachnoid hemorrhage. Neurosurgery. 2009;64:397–411.

[10] Bederson JB, Connolly Jr ES, Batjer HH, Dacey RG, Dion JE, Diringer MN, et al. Guidelines for the management of aneurysmal subarachnoid hemorrhage: a statement for healthcare professionals from a special writing group of the Stroke Council, American Heart Association. Stroke. 2009;40:994–1025.

[11] Lindegaard K-F, Nornes H, Bakke S, Sorteberg W, Nakstad P. Cerebral vasospasm diagnosis by means of angiography and blood velocity measurements. Acta neurochirurgica. 1989;100:12–24.

[12] Budohoski KP, Czosnyka M, Smielewski P, Kasprowicz M, Helmy A, Bulters D, et al. Impairment of cerebral autoregulation predicts delayed cerebral ischemia after subarachnoid hemorrhage: a prospective observational study. Stroke. 2012;43:3230–7.

[13] Budohoski KP, Czosnyka M, Smielewski P, Varsos GV, Kasprowicz M, Brady KM, et al. Cerebral autoregulation after subarachnoid hemorrhage: comparison of three methods. Journal of Cerebral Blood Flow & Metabolism. 2013;33:449–56.

[14] Nadaraya EA. On estimating regression. Theory of Probability & Its Applications. 1964;9:141–2.

[15] Watson GS. Smooth regression analysis. Sankhyā: The Indian Journal of Statistics, Series A. 1964:359–72.

[16] Placek MM, Wachel P, Czosnyka M, Soehle M, Smielewski P, Kasprowicz M. Complexity of cerebral blood flow velocity and arterial blood pressure in subarachnoid hemorrhage using time-frequency analysis. Engineering in Medicine and Biology Society (EMBC), 2015 37th Annual International Conference of the IEEE. Milan, Italy: Conf Proc IEEE Eng Med Biol Soc; 2015. p. 7700–3.

[17] Panerai RB. Cerebral autoregulation: from models to clinical applications. Cardiovascular Engineering. 2008;8:42–59.

[18] Giller CA, Mueller M. Linearity and non-linearity in cerebral hemodynamics. Medical engineering & physics. 2003;25:633–46.

[19] Mallat SG, Zhang Z. Matching pursuits with time-frequency dictionaries. IEEE Transactions on signal processing. 1993;41:3397–415.

[20] Durka PJ. From wavelets to adaptive approximations: time-frequency parametrization of EEG. BioMedical Engineering OnLine. 2003;2:1.

[21] Durka PJ, Matysiak A, Montes EM, Sosa PV, Blinowska KJ. Multichannel matching pursuit and EEG inverse solutions. Journal of neuroscience methods. 2005;148:49–59.

[22] Kuś R, Różański PT, Durka PJ. Multivariate matching pursuit in optimal Gabor dictionaries: theory and software with interface for EEG/MEG via Svarog. Biomedical engineering online. 2013;12:94.

[23] Gribonval R. Piecewise linear source separation. Wavelets: Applications in Signal and Image Processing X: International Society for Optics and Photonics; 2003. p. 297–311.

[24] Matysiak A, Durka PJ, Martinez Montes E, Barwiński M, Zwoliński P, Roszkowski M, et al. Time-frequency-space localization of epileptic EEG oscillations. Acta neurobiologiae experimentalis. 2005;65:435–42.

[25] Kordowski P, Matysiak A, König R, Sielużycki C. Simultaneous spatio-temporal matching pursuit decomposition of evoked brain responses in MEG. Biological Cybernetics. 2017;111:69–89.

[26] Czosnyka M, Brady K, Reinhard M, Smielewski P, Steiner LA. Monitoring of cerebrovascular autoregulation: facts, myths, and missing links. Neurocritical care. 2009;10:373–86.

[27] Welch PD. The use of fast Fourier transform for the estimation of power spectra: A method based on time averaging over short, modified periodograms. IEEE Transactions on audio and electroacoustics. 1967;15:70–3.

[28] Blaber AP, Bondar RL, Stein F, Dunphy PT, Moradshahi P, Kassam MS, et al. Transfer function analysis of cerebral autoregulation dynamics in autonomic failure patients. Stroke. 1997;28:1686–92.

[29] Hecht N, Fiss I, Wolf S, Barth M, Vajkoczy P, Woitzik J. Modified flow-and oxygen-related autoregulation indices for continuous monitoring of cerebral autoregulation. Journal of neuroscience methods. 2011;201:399–403.

[30] Nakagawa S, Schielzeth H. A general and simple method for obtaining R2 from generalized linear mixed-effects models. Methods in Ecology and Evolution. 2013;4:133–42.

[31] Soehle M, Czosnyka M, Pickard JD, Kirkpatrick PJ. Continuous assessment of cerebral autoregulation in subarachnoid hemorrhage. Anesthesia & Analgesia. 2004;98:1133–9.

[32] Park S, Megjhani M, Frey H-P, Grave E, Wiggins C, Terilli KL, et al. Predicting delayed cerebral ischemia after subarachnoid hemorrhage using physiological time series data. Journal of clinical monitoring and computing. 2019;33:95–105.

[33] Dineen NE, Brodie FG, Robinson TG, Panerai RB. Continuous estimates of dynamic cerebral autoregulation during transient hypocapnia and hypercapnia. Journal of applied physiology. 2010;108:604–13.

[34] Panerai RB, Dineen NE, Brodie FG, Robinson TG. Spontaneous fluctuations in cerebral blood flow regulation: contribution of PaCO2. Journal of Applied Physiology. 2010;109:1860–8.

[35] Castro PM, Santos R, Freitas J, Panerai RB, Azevedo E. Autonomic dysfunction affects dynamic cerebral autoregulation during Valsalva maneuver: comparison between healthy and autonomic dysfunction subjects. Journal of Applied Physiology. 2014;117:205–13.

[36] Liu J, Simpson MD, Yan J, Allen R. Tracking time-varying cerebral autoregulation in response to changes in respiratory PaCO2. Physiological measurement. 2010;31:1291–307.

[37] Liu J, Simpson DM, Kouchakpour H, Panerai RB, Chen J, Gao S, et al. Rapid pressure-to-flow dynamics of cerebral autoregulation induced by instantaneous changes of arterial CO2. Medical engineering & physics. 2014;36:1636–43.

[38] Giller CA. The frequency-dependent behavior of cerebral autoregulation. Neurosurgery. 1990;27:362–8.

[39] Zhang R, Zuckerman JH, Giller CA, Levine BD. Transfer function analysis of dynamic cerebral autoregulation in humans. The American journal of physiology. 1998;274:H233–41.

[40] Liu X, Donnelly J, Czosnyka M, Aries MJ, Brady K, Cardim D, et al. Cerebrovascular pressure reactivity monitoring using wavelet analysis in traumatic brain injury patients: A retrospective study. PLoS medicine. 2017;14:e1002348.

[41] Brockwell PJ, Davis RA. Estimating the Cross Spectrum: Estimation of the Phase Spectrum. Time series: theory and methods: Springer Science & Business Media; 2013. p. 448–50.

[42] Goodwin MM, Vetterli M. Matching pursuit and atomic signal models based on recursive filter banks. IEEE Transactions on Signal Processing. 1999;47:1890–902.

[43] Peng T, Rowley AB, Ainslie PN, Poulin MJ, Payne SJ. Multivariate system identification for cerebral autoregulation. Annals of biomedical engineering. 2008;36:308–20.

[44] Kostoglou K, Debert CT, Poulin MJ, Mitsis GD. Nonstationary multivariate modeling of cerebral autoregulation during hypercapnia. Medical Engineering & Physics. 2014;36:592–600.